Beam Position and Beam Hopping Design for LEO Satellite Communications

Leyi Lyu, Chenhao Qi*

School of Information Science and Engineering, Southeast University, Nanjing 210096, China
* The corresponding author, email: qch@seu.edu.cn

Cite as: L. Lyu, C. Qi, "Beam position and beam hopping design for leo satellite communications," *China Communications*, vol. 20, no. 7, pp. 29-42, 2023. **DOI**: 10.23919/JCC.fa.2023-0087.202307

Abstract: The numbers of beam positions (BPs) and time slots for beam hopping (BH) dominate the latency of LEO satellite communications. Aiming at minimizing the number of BPs subject to a predefined requirement on the radius of BP, a low-complexity user density-based BP design scheme is proposed, where the original problem is decomposed into two subproblems, with the first one to find the sparsest user and the second one to determine the corresponding best BP. In particular, for the second subproblem, a user selection and smallest BP radius algorithm is proposed, where the nearby users are sequentially selected until the constraint of the given BP radius is no longer satisfied. These two subproblems are iteratively solved until all the users are selected. To further reduce the BP radius, a duplicated user removal algorithm is proposed to decrease the number of the users covered by two or more BPs. Aiming at minimizing the number of time slots subject to the no co-channel interference (CCI) constraint and the traffic demand constraint, a low-complexity CCI-free BH design scheme is proposed, where the BPs having difficulty in satisfying the constraints are considered to be illuminated in priory. Simulation results verify the effectiveness of the proposed schemes.

Keywords: beam hopping (BH) design; beam position (BP) design; low earth orbit (LEO); low latency; satellite communications

Received: Feb. 04, 2023
Revised: Mar. 27, 2023
Editor: Zhenyu Xiao

I. INTRODUCTION

With the rapid development of the wireless technology, terrestrial communications are becoming important and popular. For densely populated areas, the architecture of terrestrial communications is almost mature. However, for some sparsely populated areas, mountains and oceans, terrestrial communications can not achieve good signal coverage [1]. To this end, we look forward to the sixth-generation wireless communications, which aims to provide ubiquitous coverage and massive user access with large communication capacity and strong reliability [2]. As a powerful complement and extension of terrestrial communications, satellite communications that are capable of providing a wide coverage, long transmission distance and flexible networking, is independent of the user environment [3]. By introducing multibeam precoding to the satellites, the energy efficiency of satellite communications can be further improved [4, 5].

In the multiuser scenarios, low earth orbit (LEO) satellite constellations are capable of providing full-time communication services without blind zones, and therefore play an important role for space-terrestrial interconnection [6]. Compared with geosynchronous earth orbit satellites and medium earth orbit satellites, LEO satellites are superior in several aspects, including power loss, propagation delay and launch cost, which makes them dominant in today's commercial

satellite communications [7]. Some new-generation large-scale LEO satellite constellations have recently been deployed, represented by SpaceX, OneWeb, Telesat and Kuiper [8–10].

With the sharp increase of demands on wireless service, the available resources on satellites become scarce. Beam hopping (BH) as a promising technology to improve the flexibility in resource allocation for satellite systems, typically uses some hopping beams to illuminate different beam positions (BPs) at different time slots so as to enlarge the whole signal coverage [11]. By simultaneously illuminating BPs that are distant from each other but keeping the other BPs non-illuminated, BH can substantially alleviate co-channel interference (CCI) [12]. Moreover, by optimizing beam illumination pattern of BH, the available resources can be allocated to match the traffic supply to the traffic demand. Given a fixed BH period, more time slots can be allocated to BPs with larger demand and lower capacity through the integer programming [13]. To further improve the dynamic adaption and reduce the computational complexity of BH, fastest queues policy (FQP) and largest queues policy (LQP) are proposed, where FQP gives priority to the fast queues and LQP gives priority to the large queues [12, 14]. Besides, considering the degree of freedom for the bandwidth, a dynamic beam pattern and bandwidth allocation scheme based on deep reinforcement learning (DRL) is proposed; and then a cooperative multi-agents DRL framework is presented, where each agent is only responsible for the illumination allocation or bandwidth allocation of a beam [15].

The latency that is an important aspect of LEO satellite communications, is mainly determined by the BH method and the number of BPs. To reduce the number of BPs, where each BP covers several users, we can set the radius of BPs variable. Aiming at minimizing the number of BPs subject to a predefined range on the radius of BP, a p-center method is presented in [16], while a heuristic method is proposed in [17] to maximize the average data rate of satellites as well as reducing the number of BPs.

The latency is mainly determined by the number of BPs and the number of time slots for BH. In this paper, we will consider minimizing the number of BPs as well as minimizing the number of time slots for BH. The main contribution of this paper is summarized as follows:

- Aiming at minimizing the number of BPs subject to a predefined requirement on the radius of BP, a low-complexity user density-based BP design (LCUD-BPD) scheme is proposed. To reduce the computational complexity, the original problem is decomposed into two subproblems, where the first subproblem is to find the sparsest user and the second one is to determine the corresponding best BP. In particular, for the second subproblem, a user selection and smallest BP radius (USSBR) algorithm is proposed to determine the best BP, where the nearby users are sequentially selected until the constraint of the given BP radius is no longer satisfied. We iteratively solve these two subproblems until all the users are selected. To further reduce the BP radius, a duplicated user removal (DUR) algorithm is proposed to decrease the number of the users covered by two or more BPs.
- Aiming at minimizing the number of time slots in LEO satellite communications subject to the traffic demand constraint and the constraint that there is no CCI between any two BPs, a low-complexity CCI-free BH design (LCCF-BHD) scheme is proposed. To reduce the computational complexity, the BPs that have difficulty in satisfying the constraints, are considered to be illuminated in priory by the LEO satellite in the LCCF-BHD scheme.

The rest of this paper is organized as follows. The considered system model for satellite communications is given in Section II. The BP design problem together with the proposed LCUD-BPD scheme is presented in Section III. The BH design problem together with the proposed LCCF-BHD scheme is presented in Section IV. Simulation results are provided in Section V. Finally, Section VI concludes this paper.

The notations used in this paper are defined as follows. Symbols for matrices (upper case) and vectors (lower case) are in boldface. $(\cdot)^{\mathrm{T}}$, $|\cdot|$, $\|\cdot\|_2$, $\mathbb{C}$, $\mathbb{R}$, $\mathbb{N}$ and $\mathcal{O}(\cdot)$ denote the transpose, absolute value, ℓ_2-norm, set of complex numbers, set of real numbers, set of positive integers, order of complexity, respectively. $[\boldsymbol{a}]_n$, $[\boldsymbol{A}]_{n,:}$, $[\boldsymbol{A}]_{:,m}$ and $[\boldsymbol{A}]_{n,m}$ denote the nth entry of vector $\boldsymbol{a}$, the nth row of matrix $\boldsymbol{A}$, the mth column of matrix $\boldsymbol{A}$, and the the entry on the nth row and mth column of matrix $\boldsymbol{A}$, respectively.

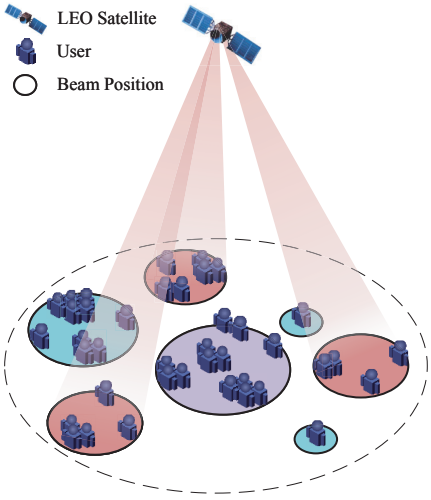

Figure 1. *Illustration of LEO satellite communications.*

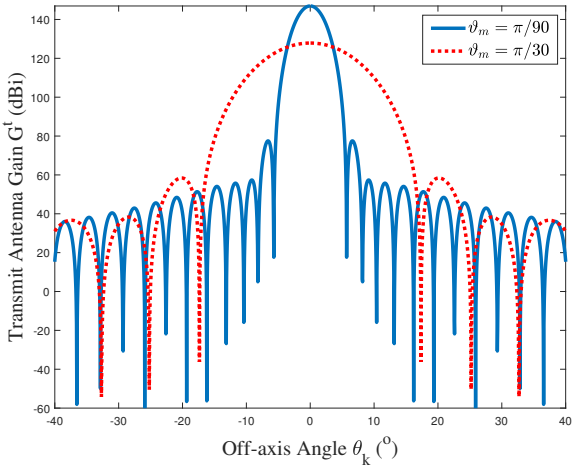

Figure 2. *Transmit antenna gain of LEO satellite for* $\vartheta_m = \pi/90$ *and* $\vartheta_m = \pi/30$.

II. SYSTEM MODEL

We consider downlink satellite communications, where a LEO satellite is used to serve K randomly distributed ground users, as shown in Figure 1. The satellite is equipped with a phased antenna array, which can form a number of spot beams and flexibly change the beam direction and beamwidth. The users are divided into M BPs based on their geographical locations, where $1 \leq M \leq K$. The number of users covered by the mth BP for $m = 1, 2, \ldots, M$ is denoted as N_m, satisfying $N_1 + N_2 + \ldots + N_M = K$. At the nth time slot for $n = 1, 2, \ldots, N_{\text{tot}}$, the satellite illuminates N_n BPs by N_n beams with $N_n \leq N_{\text{b}}$, where N_{tot} is the total number of time slots for BH and N_{b} is the maximum number of the hopping beams in each time slot. The BPs simultaneously illuminated in the same time slot are illustrated in the same color. For the users in the mth BP for $m = 1, 2, \ldots, M$, the multicast transmission is adopted [18].

Since the non-line-of-sight (NLOS) channel components are usually much weaker than the line-of-sight (LOS) channel components for satellite communications, we neglect the NLOS channel components [17]. The channel vector between the satellite and the users in the mth BP, for $m = 1, 2, \ldots, M$, is denoted by $\boldsymbol{h}_m \in \mathbb{C}^{N_m}$. The kth entry of $\boldsymbol{h}_m$, for $k = 1, 2, \ldots, N_m$, can be expressed as

$$[\boldsymbol{h}_m]_k = \alpha_{m,k} \sqrt{\left(\frac{\lambda}{4\pi d_{m,k}}\right)^2 G^{\text{r}}_{m,k} G^{\text{t}}_{m,k}}, \quad (1)$$

where $\alpha_{m,k}$ and λ denote the power attenuation of the kth user in the mth BP and the wavelength, respectively. The distance between the satellite and this user is denoted by $d_{m,k}$. The receive antenna gain of this user is denoted as $G^{\text{r}}_{m,k}$. Assuming that the hopping beams are circular, we denote the transmit antenna gain as $G^{\text{t}}_{m,k}$, which can be expressed as [19]

$$G^{\text{t}}_{m,k} = g_m \left(\frac{J_1(\mu_{m,k})}{2\mu_{m,k}} + 36 \frac{J_3(\mu_{m,k})}{\mu^3_{m,k}} \right), \quad (2)$$

where $J_1(\cdot)$ and $J_3(\cdot)$ denote the Bessel function of the first kind and the third kind, respectively. According to the convention, we define

$$\mu_{m,k} \triangleq \frac{2.07123 \sin(\theta_k)}{\sin(\vartheta_m)}, \quad (3)$$

where θ_k and ϑ_m denote the off-axis angle of the kth user and the 3dB-gain beamwidth of the mth BP in unit of angle, respectively. When $\theta_k = 0$, the achieved maximum transmit antenna gain is

$$g_m = \frac{\eta \beta^2 \pi^2}{\vartheta^2_m}, \quad (4)$$

where η denotes the antenna efficiency. β is a constant, which equals 65 for phased antenna array.

Figure 2 compares the transmit antenna gain of the satellite for $\vartheta_m = \pi/90$ and $\vartheta_m = \pi/30$. With larger

ϑ_m, g_m is smaller, but more users can be covered by the same number of BPs.

To ensure the quality of service (QoS) for the users, we assume that each beam points at the center of each BP and the users in the same BP are all located in the mainlobe of the beam [20]. Let $\boldsymbol{r} \in \mathbb{R}^M$ denote a vector including the radius of the M BPs. The radius of the mth BP, for $m = 1, 2, ..., M$, can be expressed as

$$[\boldsymbol{r}]_m = S \tan\left(\frac{\vartheta_m}{2}\right), \tag{5}$$

where S denotes the height of satellite. For each BP, its channel coefficient is defined to be that between the satellite and the worst user as [17]

$$\zeta_m \triangleq \min_k \left[|\boldsymbol{h}_m|\right]_k. \tag{6}$$

The capacity of the LEO satellite communications for the mth BP, $m = 1, 2, ..., M$, can be written as

$$C_m = B_{\text{tot}} \log_2\left(1 + \frac{P_{\text{tot}}|\zeta_m|^2}{\sigma B_{\text{tot}} N_{\text{b}}}\right), \tag{7}$$

where B_{tot}, P_{tot} and σ denote the total bandwidth, the total transmit power and the noise power spectral density, respectively. To maximize the spectral efficiency, each BP uses the whole bandwidth, while the total transmit power is uniformly allocated to the N_{b} hopping beams [16].

III. BEAM POSITION DESIGN

Note that the latency is mainly determined by the number of BPs and the number of time slots for BH. In this section, aiming at minimizing the number of BPs, we will investigate the BP design problem.

3.1 Problem Formulation

To reduce the latency, we aim to minimize the number of BPs, resulting in large radius of BPs. On one hand, larger radius of BP is capable of covering more users. On the other hand, it will lead to the transmit antenna gain of users becoming smaller, which may cause the QoS of the users to be unsatisfied in the worst case. Therefore, we aim at minimizing the number of BPs subject to a predefined requirement on the radius of BP, where the predefined requirement is essentially determined by the QoS of the users. We define $\mathcal{K} \triangleq \{1, 2, \ldots, K\}$ and $\mathcal{M} \triangleq \{1, 2, \ldots, M\}$. Then the BP design problem can be formulated as

$$\min_{\boldsymbol{X}, \boldsymbol{W}, \boldsymbol{r}} \quad M, \tag{8a}$$

$$\text{s.t.} \quad \sum_{m=1}^{M} [\boldsymbol{X}]_{m,k} \geq 1, \ \forall k \in \mathcal{K}, \tag{8b}$$

$$[\boldsymbol{r}]_m \geq r_{\min}, \ \forall m \in \mathcal{M}, \tag{8c}$$

$$[\boldsymbol{r}]_m \leq r_{\max}, \ \forall m \in \mathcal{M}, \tag{8d}$$

$$\left\|[\boldsymbol{W}]_{m,:} - [\boldsymbol{U}]_{k,:}\right\|_2 \leq [\boldsymbol{r}]_m, \quad \forall m, k \in \{m, k \mid [\boldsymbol{X}]_{m,k} = 1\}, \tag{8e}$$

where $\boldsymbol{W} \in \mathbb{R}^{M \times 2}$ and $\boldsymbol{U} \in \mathbb{R}^{K \times 2}$ denote the two-dimensional coordinates at the centers of the M BPs and the two-dimensional coordinates of the K users, respectively. We assume that the locations of the users are known to the satellite [17]. For a binary matrix $\boldsymbol{X} \in \mathbb{N}^{M \times K}$ indicating the relationship between a user and its covering BP, if the kth user is covered by the mth BP, $[\boldsymbol{X}]_{m,k} = 1$; otherwise $[\boldsymbol{X}]_{m,k} = 0$. Constraint (8b) states that to achieve the full coverage of users by the LEO satellite, each user must be covered by at least one BP. Constraint (8c) states that the minimum radius of BPs, which is denoted as

$$r_{\min} \triangleq 0.443 \frac{\lambda S}{D}, \tag{9}$$

is limited by hardware conditions, including wavelength λ, the height of satellite S and the diameter of phased antenna array D [21]. Constraint (8d) states that the maximum radius of BPs, denoted as $r_{\max}$, is a predefined requirement essentially determined by the QoS of the users. Constraint (8e) states that for each BP, its radius should be sufficient to cover all users belonging to this BP.

3.2 LCUD-BPD Scheme

Once an optimal solution, i.e., an optimal M is obtain in (8), there may be multiple solutions for $\boldsymbol{r}$, $\boldsymbol{X}$ and $\boldsymbol{W}$. In fact, since constraints (8d) and (8e) only give the upper and lower bounds of the BP radius, multiple solutions of $\boldsymbol{r}$ could be figured out. But intuitively, we prefer smaller $\boldsymbol{r}$, as smaller $\boldsymbol{r}$ leads to larger transmit

antenna gain and larger SNR of the users.

In the following, the LCUD-BPD scheme will be proposed to solve (8), where the original BP design problem is decomposed into two subproblems. The first subproblem is to find the sparsest user, and the second one is to determine the corresponding best BP. For the second subproblem, the USSBR algorithm will be proposed. These two subproblems will be iteratively solved until all the K users are selected. To further reduce BP radius, the DUR algorithm will be proposed.

3.2.1 First Subproblem to Find the Sparsest User

The users are randomly distributed in the coverage area of the LEO satellite. As shown in Figure 3, $K = 50$ ground users are randomly distributed, where the users may be close to or far from each other. Therefore, we define a distance matrix $\boldsymbol{D} \in \mathbb{R}^{K\times K}$, where the distance between the ith user and the jth user can be expressed as

$$[\boldsymbol{D}]_{i,j} = \left\|[\boldsymbol{U}]_{i,:} - [\boldsymbol{U}]_{j,:}\right\|_2, \ \forall i, j \in \mathcal{K}. \tag{10}$$

To better describe the distribution of the K users, we define the user density vector as $\boldsymbol{\rho} \in \mathbb{R}^K$, which can be expressed as

$$[\boldsymbol{\rho}]_k \triangleq \sum_{i=1}^{K} [\boldsymbol{D}]_{k,i}, \ \forall k \in \mathcal{K}. \tag{11}$$

If $[\boldsymbol{\rho}]_k$ is small, the kth user is located in a densely populated area; otherwise, the kth user is located in a sparsely populated area. Figure 3 also shows the normalized user density, where $\boldsymbol{\rho}$ is normalized by the maximum of $\boldsymbol{\rho}$. The points in dark blue represent the users in sparsely populated areas, while the points in light blue represent the users in densely populated areas.

For different users, the number of candidate BPs is different. Figure 4 shows the number of candidate BPs for different users, with the maximum radius $r_{\max} = 100\,\mathrm{km}$. For user k_1 in a sparsely populated area, there is only one candidate BP in red solid line that covers user k_1 and his nearby users. The BP in blue dashed line does not satisfy the $r_{\max}$ constraint. For user k_2 in a densely populated area, there are four candidate

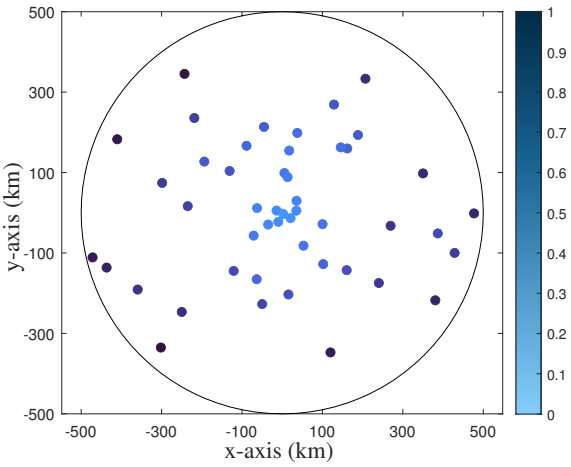

Figure 3. *Normalized density of users when $K = 50$.*

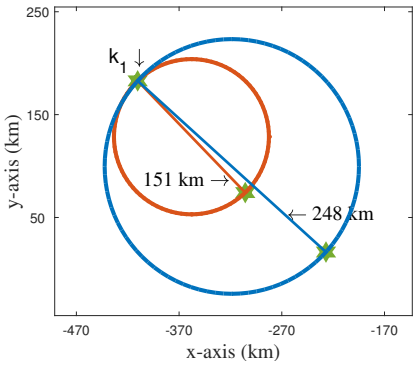

(a) *Sparsely populated area*

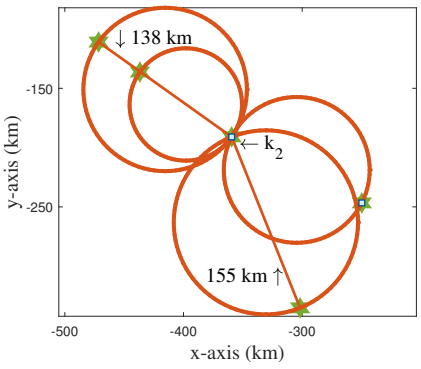

(b) *Densely populated area*

Figure 4. *Sparsely populated area and densely populated area with different numbers of candidate BPs.*

BPs. For the users in sparsely populated areas, the number of candidate BPs is small, which means that they are less likely to be covered by the same BP as other users. Therefore, the BP design scheme starts from the sparsest user, which is denoted as k_s and can

Algorithm 1. *USSBR algorithm.*

Input: $\mathcal{L}$, $\boldsymbol{U}$, $r_{\max}$, $r_{\min}$, k_{s}.
Output: $\boldsymbol{z}_{\mathrm{s}}$, ω_{s}, $\mathcal{J}_m$, $\mathcal{I}$.

Initialize $\boldsymbol{z}_{\mathrm{s}}$, ω_{s}, $\mathcal{J}_m$ and $\mathcal{I}$ via (14), (15), (16) and (17), respectively.
while $\mathcal{I} \neq \emptyset$ **do**
  Obtain $[\boldsymbol{D}]_{m,:}$ via (10).
  Find a user $\tilde{k}$ via (18) and (19).
  Update $\mathcal{J}_m$ via (20).
  Obtain $\boldsymbol{z}$, ω using randomized algorithm.
  if $\omega \leq r_{\max}$ **then**
    Update $\boldsymbol{z}_{\mathrm{s}}$ and ω_{s} via (21).
  else
    Update $\mathcal{J}_m$ and $\mathcal{I}$ via (22).
    Break.
  end if
end while

be determined by

$$k_{\mathrm{s}} = \arg\max_{k \in \mathcal{L}} [\boldsymbol{\rho}]_k, \tag{12}$$

where $\mathcal{L}$ denotes the set of remaining users during the total iterative BP design and is initialized to be $\mathcal{K}$ as

$$\mathcal{L} \leftarrow \mathcal{K}. \tag{13}$$

3.2.2 Second Subproblem to Determine the Best BP

Once the sparsest user k_{s} is determined, we need to determine the corresponding best BP.

When designing the mth BP, its center coordinates, which is denoted as $\boldsymbol{z}_{\mathrm{s}} \in \mathbb{R}^2$, is initialized by

$$\boldsymbol{z}_{\mathrm{s}} \leftarrow [\boldsymbol{U}]_{k_{\mathrm{s}},:}, \tag{14}$$

where the center coordinates of the mth BP $\boldsymbol{z}_{\mathrm{s}}$ is set to be the coordinates of user k_{s}. The radius of the mth BP, which is denoted as ω_{s}, is initialized by

$$\omega_{\mathrm{s}} \leftarrow r_{\min}. \tag{15}$$

The set including the user k_{s} and his nearby users covered by the mth BP, is denoted as $\mathcal{J}_m$, which is initialized as

$$\mathcal{J}_m \leftarrow \{k_{\mathrm{s}}\}. \tag{16}$$

Algorithm 2. *LCUD-BPD scheme.*

Input: $\mathcal{K}$, $\boldsymbol{U}$, $r_{\max}$, $r_{\min}$.
Output: $\boldsymbol{W}$, $\boldsymbol{r}$, $\boldsymbol{X}$, M.

Initialize m, $\boldsymbol{W}$, $\boldsymbol{r}$ and $\boldsymbol{X}$ via (23), and initialize $\mathcal{L}$ via (13).
Obtain user density $\boldsymbol{\rho}$ via (11).
while $\mathcal{L} \neq \emptyset$ **do**
  $m \leftarrow m + 1$.
  Obtain the user k_{s} via (12).
  Obtain $\boldsymbol{z}_{\mathrm{s}}$, ω_{s}, $\mathcal{J}_m$, $\mathcal{I}$ via **Algorithm** 1.
  Update $\boldsymbol{W}$, $\boldsymbol{r}$ and $\mathcal{L}$ via (24), and update $\boldsymbol{X}$ via (26).
end while
$M \leftarrow m$.

The set of remaining users during the iterative BP design, denoted as $\mathcal{I}$, is initialized to be $\mathcal{L}$ as

$$\mathcal{I} \leftarrow \mathcal{L}. \tag{17}$$

We compute the distance between the center of the mth BP and the users in $\mathcal{I}$ via (10). Then we find the user $\tilde{k}$, which is most likely to be covered together with the users in $\mathcal{J}_m$ by the mth BP. Therefore, $\tilde{k}$ should satisfy the following constraints

$$[\boldsymbol{D}]_{m,\tilde{k}} > [\boldsymbol{r}]_m, \tag{18}$$

$$[\boldsymbol{D}]_{m,\tilde{k}} \leq [\boldsymbol{D}]_{m,i}, \ \forall i \in \mathcal{I} \backslash \mathcal{J}_m. \tag{19}$$

In fact, constraint (18) indicates that user $\tilde{k}$ has not yet been covered by the mth BP. Constraint (19) states that except for the users that have already been covered by the mth BP, user $\tilde{k}$ is closest to the center of the mth BP. Then we update $\mathcal{J}_m$ by

$$\mathcal{J}_m \leftarrow \mathcal{J}_m \cup \{\tilde{k}\}. \tag{20}$$

To cover all the users in $\mathcal{J}_m$, the BP with the smallest radius is determined by the randomized algorithm [22], where the obtained center coordinates and the radius of the BP are denoted as $\boldsymbol{z} \in \mathbb{R}^2$ and ω, respectively. If constraint (8d) is satisfied, i.e., $\omega \leq r_{\max}$, we update the center coordinates and the radius of the mth BP to be $\boldsymbol{z}$ and ω as

$$\boldsymbol{z}_{\mathrm{s}} \leftarrow \boldsymbol{z}, \ \omega_{\mathrm{s}} \leftarrow \omega, \tag{21}$$

respectively. In this way, the nearby users are sequentially selected until the constraint of the given BP radius is not satisfied or there are no users to be selected. If constraint (8d) is not satisfied, we remove user $\tilde{k}$ from $\mathcal{J}_m$ and update $\mathcal{I}$ by

$$\mathcal{J}_m \leftarrow \mathcal{J}_m \backslash \tilde{k},\ \mathcal{I} \leftarrow \mathcal{I} \backslash \mathcal{J}_m, \tag{22}$$

respectively.

These steps of solving the second subproblem to determine the best BP, named the USSBR algorithm, are summarized in **Algorithm** 1. The number of iterations in **Algorithm** 1 is relevant to user distribution, the number of users in $\mathcal{I}$ and the maximum radius.

Finally, by integrating the steps to solve the first and the second subproblems, we propose the LCUD-BPD scheme, which is summarized in **Algorithm** 2.

We first initialize the iteration counter, the center coordinates matrix of the M BPs, the radius vector of the M BPs, and the binary matrix indicating the relationship between a user and its covered BP as

$$m \leftarrow 0,\ \boldsymbol{W} \leftarrow \emptyset,\ \boldsymbol{r} \leftarrow \emptyset,\ \boldsymbol{X} \leftarrow \emptyset, \tag{23}$$

respectively.

By obtaining the user k_{s} via (12), we solve the first subproblem to find the sparsest user. By obtaining $\boldsymbol{z}_{\mathrm{s}}$, ω_{s}, $\mathcal{J}_m$, $\mathcal{I}$ via **Algorithm** 1, we solve the second subproblem to determine the best BP. Then we update $\boldsymbol{W}$, $\boldsymbol{r}$ and $\mathcal{L}$ as

$$\boldsymbol{W} \leftarrow [\boldsymbol{W}^{\mathrm{T}}, \boldsymbol{z}_{\mathrm{s}}]^{\mathrm{T}},\ \boldsymbol{r} \leftarrow [\boldsymbol{r}^{\mathrm{T}}, \omega_{\mathrm{s}}]^{\mathrm{T}},\ \mathcal{L} \leftarrow \mathcal{I}, \tag{24}$$

respectively. To update $\boldsymbol{X}$, we first introduce a temporary zero vector $\boldsymbol{x} \leftarrow \boldsymbol{0}^K$, then set

$$[\boldsymbol{x}]_k \leftarrow 1,\ \forall k \in \mathcal{J}_m, \tag{25}$$

and finally update $\boldsymbol{X}$ by

$$\boldsymbol{X} \leftarrow [\boldsymbol{X}^{\mathrm{T}}, \boldsymbol{x}]^{\mathrm{T}}. \tag{26}$$

These two subproblems will be iteratively solved until all the K users are selected, i.e. $\mathcal{L} = \emptyset$. In fact, the number of iterations for **Algorithm** 2 is M.

To further reduce the BP radius, the DUR algorithm will be proposed in the following.

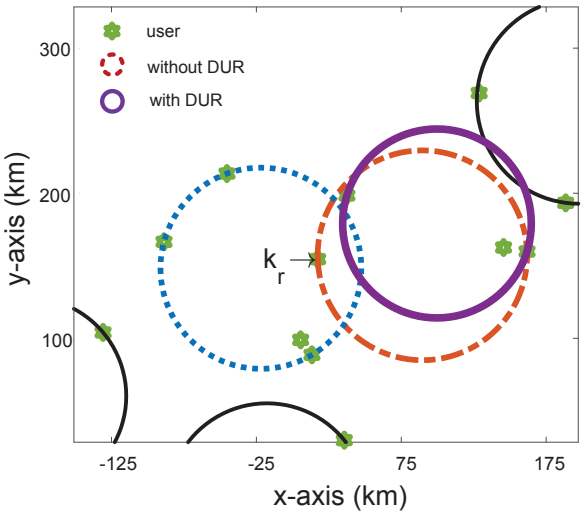

Figure 5. *Illustration of DUR.*

3.2.3 Duplicated User Removal

Since we select the users in order, some users may be covered by two or more BPs. As shown in Figure 5, we suppose that the BP illustrated by the red circle is determined first. Then all the users covered by the red circle are removed from $\mathcal{I}$, including user k_{r}. To cover the remaining users in $\mathcal{I}$, the BP illustrated by the blue circle is then determined; but user k_{r} is covered again. In fact, user k_{r} can solely be covered by the blue circle, which can lead to a smaller radius of the red circle. Therefore, user k_{r} is named as a duplicated user, and such an operation is called DUR. After DUR, the BP with a smaller radius is illustrated in a purple circle.

To perform DUR, we first define an iteration counter t that is initialized as

$$t \leftarrow 1. \tag{27}$$

Then we define a matrix indicating the center coordinates of the M BPs at the tth iteration as $\boldsymbol{W}^t$, which is initialized as

$$\boldsymbol{W}^t \leftarrow \boldsymbol{W}. \tag{28}$$

Similarly, we define a radius vector of the M BPs at the tth iteration as $\boldsymbol{r}^t$, which is initialized as

$$\boldsymbol{r}^t \leftarrow \boldsymbol{r}. \tag{29}$$

The duplicated user k_{r} is determined by

$$[\boldsymbol{D}]_{m,k_{\mathrm{r}}} \leqslant [\boldsymbol{r}]_m,\ k_{\mathrm{r}} \notin \mathcal{J}_m,\ \forall m \in \mathcal{M}. \tag{30}$$

By classifying the duplicated user k_{r} to the nearest BP, the number of duplicated users can be reduced, where the nearest BP is determined by

$$\tilde{m} = \arg\min_{m \in \mathcal{M}} \left\| [\boldsymbol{U}]_{k_{\mathrm{r}},:} - [\boldsymbol{W}]_{m,:} \right\|_2. \tag{31}$$

Note that $\tilde{m}$ is the index of the BP that will cover the user k_{r} after DUR. Then we update $\boldsymbol{X}$ by

$$[\boldsymbol{X}]_{\hat{m},k} \leftarrow 0,\ [\boldsymbol{X}]_{\tilde{m},k} \leftarrow 1, \tag{32}$$

where $\hat{m}$ is the index of the BP covering the duplicate user k_{r} before DUR. For the $\hat{m}$th BP, the radius and the corresponding center coordinates after DUR are determined by the randomized algorithm, and are denoted as $\boldsymbol{z}_{\hat{m}}$ and $\omega_{\hat{m}}$, respectively. Then we update $\boldsymbol{W}^t$ and $\boldsymbol{r}^t$ by

$$[\boldsymbol{W}^t]_{\hat{m},:} \leftarrow \boldsymbol{z}_{\hat{m}}^{\mathrm{T}},\ [\boldsymbol{r}^t]_{\hat{m}} \leftarrow \omega_{\hat{m}}, \tag{33}$$

respectively.

We repeat the above steps until the center coordinates of the M BPs obtained in current iteration are exactly the same as those in the previous iteration, i.e., $\boldsymbol{W}^t = \boldsymbol{W}^{t-1}$. The detailed steps of the proposed DUR algorithm are summarized in **Algorithm** 3. Note that Algorithm 3 needs to be performed based on the output of **Algorithm** 2.

Algorithm 3. *DUR algorithm.*

Input: $\mathcal{K}, \boldsymbol{U}, \boldsymbol{W}, \boldsymbol{r}, \boldsymbol{X}, M, r_{\max}, r_{\min}$.
Output: $\boldsymbol{W}, \boldsymbol{r}, \boldsymbol{X}, M$.
1: Initialize t, $\boldsymbol{W}^t$ and $\boldsymbol{r}^t$ via (27), (28) and (29), respectively.
2: **while** $\boldsymbol{W}^t \neq \boldsymbol{W}^{t-1}$ **do**
3: Determine k_{r} via (30).
4: Determine $\tilde{m}$ via (31).
5: Update $\boldsymbol{X}$ via (32).
6: Obtain $\boldsymbol{z}_{\hat{m}}$ and $\omega_{\hat{m}}$ using the randomized algorithm.
7: Update $\boldsymbol{W}^t$ and $\boldsymbol{r}^t$ via (33).
8: $t \leftarrow t + 1$.
9: **end while**
10: $\boldsymbol{W} \leftarrow \boldsymbol{W}^t, \boldsymbol{r} \leftarrow \boldsymbol{r}^t$.

3.2.4 Computational Complexity Analysis

It can be observed that **Algorithm** 2 needs M outer iterations. During each outer iteration, **Algorithm** 1 needs at most T_2 inner iterations, where T_2 is relevant to user distribution, the number of users in $\mathcal{I}$ and the maximum radius. During each inner iteration, the computational complexity is no higher than $\mathcal{O}(K)$ on computing the distance between the center of a BP and the K users. Therefore, the total computational complexity of **Algorithm** 2 is $\mathcal{O}(MT_2K)$.

The computational complexity of **Algorithm** 3 is $\mathcal{O}(T_3 M_{\mathrm{r}} K)$, where T_3 and M_r denote the number of iterations and the number of duplicated users, respectively. Since $T_3 \ll T_{\max}$ and $M_{\mathrm{r}} \ll M$, the computational complexity of **Algorithm** 3 is much lower than **Algorithm** 2. As a result, the total computational complexity of the LCUD-BPD scheme with DUR in solving (8) is $\mathcal{O}(MT_2K)$.

As a comparison, the computational complexity of the existing p-center method and user grouping method is $\mathcal{O}\left(K^2(K-1)/2\right)$ [23] and $\mathcal{O}(T_{\mathrm{u}}KM)$ [17], respectively, where T_{u} is the number of iterations. The numerical comparisons for our proposed scheme and the existing methods will be included in Section V.

IV. BEAM HOPPING DESIGN

To further reduce the latency, in this section, aiming at minimizing the number of time slots for BH, we will investigate the BH design problem.

4.1 CCI-Free Constraint

In the coverage area of the LEO satellite, some BPs are adjacent. If these BPs are simultaneously illuminated, CCI would seriously affect the SNR. The BH allows the adjacent BPs to be illuminated at different time slot to completely eliminate the CCI, while the BPs far from each other without any CCI are illuminated within the same time slot.

The CCI-free distance between any two BPs is denoted as $\boldsymbol{B} \in \mathbb{R}^{M \times M}$. If the distance between the ith

BP and the jth BP is no smaller than 6 times of the radius of the jth BP, the CCI from the jth BP is considered to be completely eliminated for the ith BP [24]. Similarly, if the distance between the ith BP and the jth BP is no smaller than 6 times of the radius of the ith BP, the CCI from the ith BP is considered to be completely eliminated for the jth BP. Therefore, the CCI-free distance between the ith BP and the jth BP is determined by

$$[\boldsymbol{B}]_{i,j} = 6\max\left\{[\boldsymbol{r}]_i, [\boldsymbol{r}]_j\right\},\ i \neq j,\ \forall i,j \in \mathcal{M}. \quad (34)$$

The distance between any two BPs, is represented by a matrix $\boldsymbol{P} \in \mathbb{R}^{M\times M}$, where $[\boldsymbol{P}]_{i,j}$ denotes the distance between the center of the ith BP and the center of the jth BP. Note that $\boldsymbol{P}$ can be obtained by (10) if we replace the users by the BPs. We define a binary interference matrix as $\boldsymbol{Q} \in \mathbb{N}^{M\times M}$, which can be determined by

$$[\boldsymbol{Q}]_{i,j} = \begin{cases} 1, & [\boldsymbol{P}]_{i,j} < [\boldsymbol{B}]_{i,j} \\ 0, & [\boldsymbol{P}]_{i,j} \geq [\boldsymbol{B}]_{i,j} \end{cases}. \quad (35)$$

If $[\boldsymbol{Q}]_{i,j} = 1$, there is CCI between the ith BP and the jth BP; otherwise, there is no CCI.

4.2 Problem Formulation

The total traffic demand of the M BPs, denoted as $\boldsymbol{d} \in \mathbb{R}^M$, is normally known to the satellite [13]. We define L as the duration of one time slot. Then we denote the traffic supply of the M BPs in L as $\boldsymbol{s} \in \mathbb{R}^M$, whose mth entry indicating the traffic supply of the mth BP in L can be expressed as

$$[\boldsymbol{s}]_m = LC_m,\ \forall m \in \mathcal{M}. \quad (36)$$

The definition of C_m is given in (7). To satisfy the traffic demand of the M BPs, the numbers of time slots with illumination are represented by a vector $\boldsymbol{b} \in \mathbb{N}^M$, with its mth entry defined as

$$[\boldsymbol{b}]_m = \left\lceil \frac{[\boldsymbol{d}]_m}{[\boldsymbol{s}]_m} \right\rceil,\ \forall m \in \mathcal{M}, \quad (37)$$

where $\lceil\cdot\rceil$ denotes the ceiling operation. We define $\mathcal{N} \triangleq \{1, 2, \ldots, N\}$. Aiming at minimizing the number of time slots for BH subject to the CCI-free constraint and traffic demand constraint, the BH design problem can be formulated as

$$\min_{\boldsymbol{N}} \quad N_{\text{tot}}, \quad (38a)$$

$$\text{s.t.} \quad \sum_{n=1}^{N_{\text{tot}}} [\boldsymbol{N}]_{m,n} = [\boldsymbol{b}]_m,\ \forall m \in \mathcal{M}, \quad (38b)$$

$$\sum_{m=1}^{M} [\boldsymbol{N}]_{m,n} \leqslant N_{\text{b}},\ \forall n \in \mathcal{N}, \quad (38c)$$

$$[\boldsymbol{N}]_{:,n}^{\text{T}} \boldsymbol{Q} [\boldsymbol{N}]_{:,n} = 0,\ \forall n \in \mathcal{N}. \quad (38d)$$

For the binary matrix $\boldsymbol{N} \in \mathbb{N}^{M\times N_{\text{tot}}}$ indicating the relationship between a BP and its illuminated time slot, if the mth BP is illuminated at the nth time slot, $[\boldsymbol{N}]_{m,n} = 1$; otherwise, $[\boldsymbol{N}]_{m,n} = 0$. Constraint (38b) states that the traffic demand of all M BPs must be satisfied. Constraint (38c) provides the maximum number of hopping beams N_{b} that can be simultaneously illuminated. Constraint (38d) states that there is no CCI between any two BPs.

In the following, we will propose the LCCF-BDH scheme to solve (38).

4.3 LCCF-BDH Scheme

For the BPs with a large radius in a densely populated area, the CCI-free constraint is difficult to satisfy, since the number of its partner BPs that can be simultaneously illuminated without any CCI is small. However, for the BPs with a small radius in a sparsely populated area, the CCI-free constraint is much easier to satisfy, since the number of its partner BPs that can be simultaneously illuminated without any CCI is large. Therefore, the BPs with a large radius in a densely populated area will be considered in priory. Similarly, the BPs with a large number of time slots indicated by $\boldsymbol{b}$ needs to be considered in priory.

We denote the selection priority vector as $\boldsymbol{\varsigma} \in \mathbb{N}^M$, with its mth entry expressed as

$$[\boldsymbol{\varsigma}]_m \triangleq \frac{[\boldsymbol{q}]_m}{2\max(\boldsymbol{q})} + \frac{[\boldsymbol{b}]_m}{2\max(\boldsymbol{b})},\ \forall m \in \mathcal{M}, \quad (39)$$

where $\boldsymbol{q} \in \mathbb{N}^M$ denotes the the number of BPs that can be simultaneously illuminated without any CCI.

To start the LCCF-BHD scheme, we define a set including the indices of the remaining BPs as $\mathcal{F}$, which is initialized to be $\mathcal{M}$ as

$$\mathcal{F} \leftarrow \mathcal{M}. \tag{40}$$

Then we define an iteration counter n that is initialized as

$$n \leftarrow 0. \tag{41}$$

We define the set including the BPs illuminated at the nth time slot as $\mathcal{P}_n$, which is initialized by

$$\mathcal{P}_n \leftarrow \emptyset. \tag{42}$$

We initialize $\boldsymbol{N}$ by

$$\boldsymbol{N} \leftarrow \emptyset. \tag{43}$$

In the nth time slot, we determine $\boldsymbol{\varsigma}$ via (39). The largest entry in $\boldsymbol{\varsigma}$ is considered to be illuminated with the highest priority. We determine the index of the largest entry in $\boldsymbol{\varsigma}$ by

$$i = \arg\max_{l \in \mathcal{M}} \ [\boldsymbol{\varsigma}]_l. \tag{44}$$

Then we update $\boldsymbol{\varsigma}$ by setting its ith entry zero as

$$[\boldsymbol{\varsigma}]_i \leftarrow 0. \tag{45}$$

If the ith BP cannot satisfy the CCI-free constraint with any BP in $\mathcal{P}_n$, we will not illuminate this BP and never consider it in the same time slot; otherwise, i.e., $[\boldsymbol{Q}]_{i,j} = 0, \forall j \in \mathcal{P}_n$, we update $\boldsymbol{b}$ and $\mathcal{P}_n$ by

$$[\boldsymbol{b}]_i \leftarrow [\boldsymbol{b}]_i - 1, \ \mathcal{P}_n \leftarrow \mathcal{P}_n \cup i, \tag{46}$$

respectively.

These steps are iteratively performed until the number of illuminated BPs equals N_b, i.e., $P = N_\mathrm{b}$, or all entries of (39) are zero, i.e., $\boldsymbol{\varsigma} = \boldsymbol{0}^M$. After iteratively processing the BPs in the nth time slot, we update $\mathcal{F}$ by removing the BPs that have been satisfied with the traffic demand as

$$\mathcal{F} \leftarrow \mathcal{F} \backslash \{l \mid [\boldsymbol{b}]_l = 0\}. \tag{47}$$

Algorithm 4. *LCCF-BHD scheme.*

Input: $\mathcal{M}$, $\boldsymbol{W}$, $\boldsymbol{r}$, $\boldsymbol{q}$, $\boldsymbol{b}$, M.
Output: N_tot.

```
Initialize F, n, P_n and N via (40), (41), (42) and (43), respectively.
while F ≠ ∅ do
    n ← n + 1, p ← 0.
    Obtain ς via (39).
    while p < N_b or ς ≠ 0^M do
        Determine i via (44).
        Update ς by (45).
        if [Q]_{i,j} = 0, ∀j ∈ P_n then
            Update b and P_n via (46).
            p ← p + 1.
        end if
    end while
    Update F via (47) and N via (49).
end while
N_tot ← n.
```

To update $\boldsymbol{N}$ with the results from the nth time slot, we first introduce a temporary zero vector $\boldsymbol{n} \leftarrow \boldsymbol{0}^M$, then set

$$[\boldsymbol{n}]_i \leftarrow 1, \forall i \in \mathcal{P}_n, \tag{48}$$

and finally update $\boldsymbol{N}$ by

$$\boldsymbol{N} \leftarrow [\boldsymbol{N}, \boldsymbol{n}]. \tag{49}$$

We repeat these steps until the traffic demand constraint is satisfied, i.e., $\mathcal{F} = \emptyset$. The detailed steps of the proposed LCCF-BHD scheme are summarized in **Algorithm** 4. The output of **Algorithm** 4 is a solution to (38).

4.4 Computational Complexity Analysis

It can be observed that **Algorithm** 4 needs N_tot outer iterations. During each outer iteration, at most M inner iterations is needed. During each inner iteration, the computational complexity is no higher than $\mathcal{O}(N_\mathrm{b})$ on determining whether CCI-free constraint is satisfied. As a result, the total computational complexity of the LCCF-BHD scheme in solving (38) is $\mathcal{O}\left(N_\mathrm{tot} M N_\mathrm{b}\right)$. As a comparison, the computational complexity of the existing CVX method and ICS method is $\mathcal{O}\left({N_\mathrm{c}}^{b_\mathrm{max}}\right)$ [13] and $\mathcal{O}\left(N_\mathrm{I} M N_\mathrm{b}\right)$ [14],

Table 1. *Simulation parameters.*

Symbols	Definition	Value
S	The height of satellite	1000 km
P_{tot}	Total transmit power	100 W
B_{tot}	Total bandwidth	240 MHz
N_{b}	Maximum number of hopping beams	4
L	Duration of one time slot	2 ms
$r_{\max}$	Maximum radius of BP	100 km
$r_{\min}$	Minimum radius of BP	24 km
$G^{\text{r}}_{m,k}$	Receive antenna gain	40 dBi

where N_{c}, $b_{\max} \triangleq \max_{m\in\mathcal{M}}[\boldsymbol{b}]_m$ and N_{I} denote the number of all available CCI-free combinations, the maximum number of time slots with illumination and the number of iterations of the ICS method, respectively. The numerical comparisons for our proposed scheme and the existing methods will be included in Section V.

V. SIMULATION RESULTS

In this section, we evaluate both the performance and the computational complexity for the LCUD-BPD scheme and the LCCF-BHD scheme, where the performance metrics include the minimum number of BPs, the average BP radius and the minimum number of time slots. A LEO satellite working at 20GHz Ka band covers an area with the radius of 500km on the ground [16]. The parameters for the simulation are provided in Table 1.

5.1 Performance and Complexity Evaluation for LCUD-BPD Scheme

Now we evaluate both the performance and the computational complexity for the LCUD-BPD scheme. Figure 6 compares the minimum number of BPs, denoted by M in (8a), obtained by the LCUD-BPD scheme, p-center method [16] and user grouping method [17], when the number of users increases from $K = 25$ to $K = 200$. It is seen that both the LCUD-BPD scheme and the p-center method perform much better than the user grouping method. As K increases, three curves all climb. When we increase from $K = 50$ to $K = 200$, the performance reduction of the LCUD-BPD scheme over the p-center method

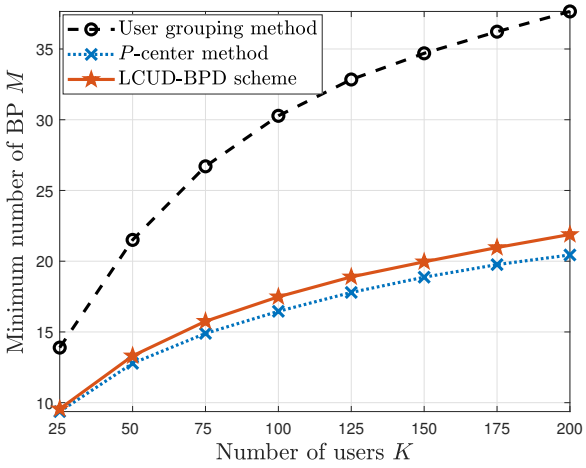

Figure 6. *Comparison of the minimum number of BPs for different numbers of users.*

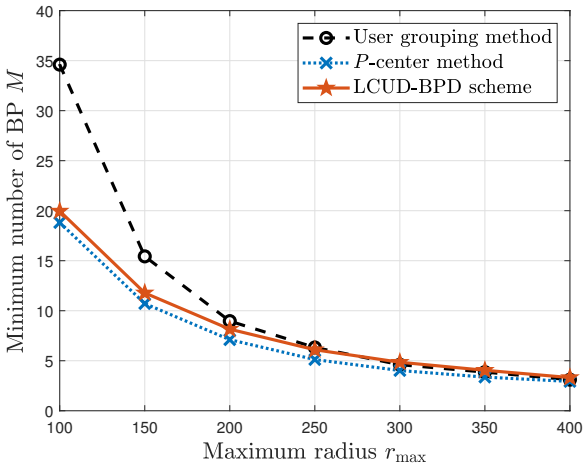

Figure 7. *Comparison of the minimum number of BPs for different maximum radius.*

grows from 4.13% to 7.07%; however, the sacrifice of the computational complexity is much larger, i.e., the reduction in computational complexity of the LCUD-BPD scheme over the p-center method grows from 89.13% to 97.8% according to Section 3.2.4. Moreover, we also compare the running time for the LCUD-BPD scheme and the p-center method using the same computer hardware and software. When we set $K = 200$, the running time for the LCUD-BPD scheme and the p-center method is 0.0206s and 10.8081s, respectively, which results in 99.8% reduction in computational complexity of the LCUD-BPD scheme over the p-center method.

Figure 7 compares the minimum number of BPs, de-

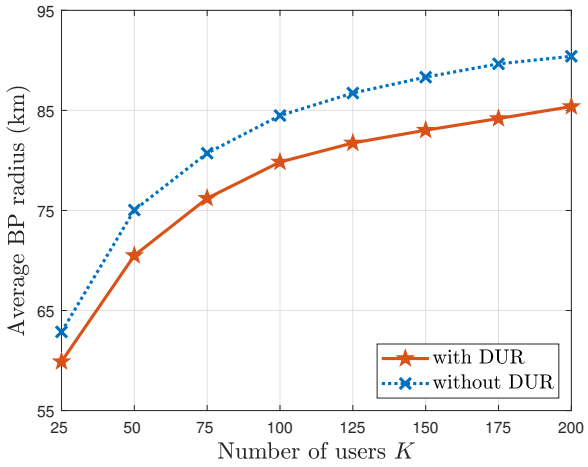

Figure 8. *Comparisons of the average BP radius using LCUD-BPD with DUR and without DUR.*

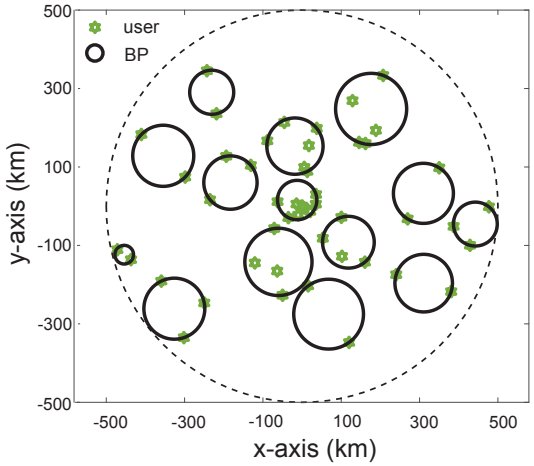

Figure 9. *Illustration of the BP design results using LCUD-BPD with DUR for $K = 50$.*

termined by M in (8a), obtained by the LCUD-BPD scheme, p-center method and user grouping method when the number of users is fixed to be $K = 150$ and the maximum radius of BPs increases from $r_{\max} = 100$ to $r_{\max} = 400$. It is seen that both the LCUD-BPD scheme and the p-center method perform better than the user grouping method. As $r_{\max}$ increases, three curves all decline and the performance gap in terms of M between any two curves gets small. Note that if $r_{\max}$ grows to be 500, which equals the radius of the coverage area of the LEO satellite, three curves will all result in $M = 1$.

Then we evaluate the performance of the DUR algorithm. Figure 8 compares the average BP radius, obtained by the LCUD-BPD scheme with DUR algorithm and without DUR algorithm for different numbers of users. When we increase K, the average BP radius grows, indicating that the BP radius can be more sufficiently used to minimize M. It is seen that with DUR algorithm, the average BP radius is smaller than that without DUR algorithm. When we increase from $K = 25$ to $K = 200$, the performance improvement of the LCUD-BPD scheme with DUR algorithm over that without DUR algorithm grows from 2.97 km to 5.02 km, which verifies the effectiveness of the DUR algorithm and implies that it works better for larger K. Figure 9 illustrates the BP design results with the DUR algorithm if we set $K = 50$ and $r_{\max} = 100$. It is seen that we can get $M = 14$, where the largest and smallest radius of the designed BPs are 90.74 km and 24km, respectively, and the average BP radius is 70.81km.

5.2 Performance and Complexity Evaluation for LCCF-BHD Scheme

Now we evaluate both the performance and the computational complexity of the LCCF-BHD schemes. Since the performance of the LCUD-BPD scheme and p-center method is similar while the complexity of the former is much smaller than the latter, in this subsection we first use the LCUD-BPD scheme to determine the minimum number of BPs, including the center coordinates and the radius of these BPs, and then consider the BH design problem in (38). In fact, (38) is an integer programming problem, which can be solved by CVX integer programming solution package [25].

Figure 10 compares the minimum number of total time slots, denoted as N_{tot} in (38a), obtained by the LCCF-BHD scheme, CVX method [13] and ICS method [14] for different numbers of users. As shown in Table 1, the maximum number of the hopping beams in the same time slot is set to be $N_{\text{b}} = 4$. The number of time slots with illumination to satisfy the traffic demand of the mth BP, denoted as $[\boldsymbol{b}]_m$, for $m = 1, 2, \ldots, M$, is randomly generated from the integer set $\{1, 2, 3\}$, i.e., $b_{\max} = 3$. It is seen that as K increases, three curves all climb, indicating that more users needs more time slots to satisfy their traffic demand. Moreover, both the LCCF-BHD scheme and CVX method perform much better than the ICS

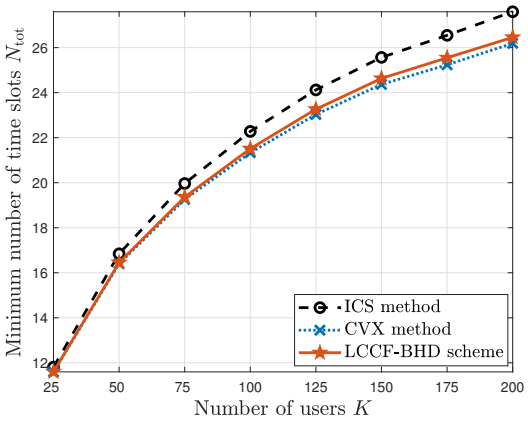

Figure 10. *Comparison of the minimum number of time slots for LCCF-BHD and the existing methods for different users.*

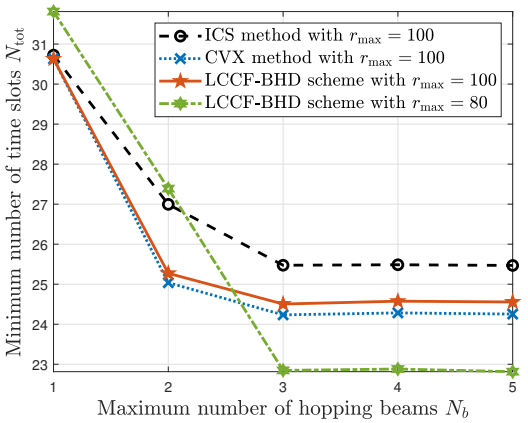

Figure 11. *Comparison of the minimum number of time slots for LCCF-BHD and the existing methods for different maximum number of hopping beams.*

method. When we increase from $K = 25$ to $K = 200$, the performance reduction of the LCCF-BHD scheme over the CVX method grows from 0.06% to 1.02%; however, the sacrifice of the computational complexity is much larger, i.e., the reduction in computational of the LCCF-BHD scheme over the CVX method is 99.9% according to Section 4.4. In addition, we also compare the running time for the LCCF-BHD scheme and the CVX method using the same computer hardware and software. When setting $K = 200$, the running time for the LCCF-BHD scheme and the CVX method is 0.0138s and 19.8143s, respectively, which results in 99.9% reduction in computational complexity of the LCCF-BHD scheme over the CVX method.

Figure 11 compares the minimum number of total time slots, denoted as $N_{\rm tot}$ in (38a), obtained by the LCCF-BHD scheme, CVX method and ICS method for different maximum number of the hopping beams. We fix $K = 150$. It is seen that as $N_{\rm b}$ increases, four curves all decline, indicating that $N_{\rm tot}$ can be effectively reduced if large $N_{\rm b}$ is available. Note that $N_{\rm b}$ is essentially determined by the phased antenna array. As we increase from $N_{\rm b} = 1$ to $N_{\rm b} = 5$, the curves get flat and converge. The reason is that although larger $N_{\rm b}$ is available, the CCI-free constraint restricts the number of BPs that can be simultaneously illuminated within the same time slot. In this context, we need to decrease the maximum radius of BP. For $N_{\rm b} = 3$, if we further decrease the maximum radius of BP from $r_{\max} = 100$ to $r_{\max} = 80$, we can reduce from $N_{\rm tot} = 24.505$ to $N_{\rm tot} = 22.847$, which effectively saves the time slots for BH.

VI. CONCLUSION

In this paper, aiming at minimizing the number of BPs subject to a predefined requirement on the radius of BP, we have proposed the LCUD-BPD scheme. To further reduce the BP radius, we have proposed the DUR algorithm to decrease the number of the users covered by two or more BPs. Aiming at minimizing the number of time slots subject to the CCI-free constraint and the traffic demand constraint, we have proposed the LCCF-BHD scheme. Simulation results have shown that the proposed schemes can substantially reduce the complexity with little performance sacrifice compared to the existing methods. Future research includes developing algorithms for resource allocation and BH design to shorten the latency as well as reducing the mismatch between traffic supply and traffic demand.

ACKNOWLEDGEMENT

This work was supported in part by National Key Research and Development Program of China under Grant 2021YFB2900404.

References

[1] X. Fang, W. Feng, *et al.*, "5g embraces satellites for 6g ubiquitous iot: Basic models for integrated satellite terrestrial

networks," *IEEE Internet of Things Journal*, vol. 8, no. 18, pp. 14 399–14 417, 2021.
[2] Z. Xiao, J. Yang, *et al.*, "Leo satellite access network (leosan) towards 6g: Challenges and approaches," *IEEE Wireless Communications*, pp. 1–8, 2022.
[3] A. Guidotti, A. Vanelli-Coralli, *et al.*, "Architectures and key technical challenges for 5g systems incorporating satellites," *IEEE Transactions on Vehicular Technology*, vol. 68, no. 3, pp. 2624–2639, 2019.
[4] C. Qi, Y. Yang, *et al.*, "Multibeam satellite communications with energy efficiency optimization," *IEEE Communications Letters*, vol. 26, no. 4, pp. 887–891, 2022.
[5] C. Qi and X. Wang, "Precoding design for energy efficiency of multibeam satellite communications," *IEEE Communications Letters*, vol. 22, no. 9, pp. 1826–1829, 2018.
[6] B. Di, L. Song, *et al.*, "Ultra-dense leo: Integration of satellite access networks into 5g and beyond," *IEEE Wireless Communications*, vol. 26, no. 2, pp. 62–69, 2019.
[7] Z. Qu, G. Zhang, *et al.*, "Leo satellite constellation for internet of things," *IEEE access*, vol. 5, pp. 18 391–18 401, 2017.
[8] A. Lalbakhsh, A. Pitcairn, *et al.*, "Darkening low-earth orbit satellite constellations: A review," *IEEE Access*, vol. 10, pp. 24 383–24 394, 2022.
[9] J. C. McDowell, "The low earth orbit satellite population and impacts of the spacex starlink constellation," *The Astrophysical Journal Letters*, vol. 892, no. 2, pp. 36–45, 2020.
[10] S. Xia, Q. Jiang, *et al.*, "Beam coverage comparison of leo satellite systems based on user diversification," *IEEE Access*, vol. 7, pp. 181 656–181 667, 2019.
[11] J. Lei and M. A. Vazquez-Castro, "Multibeam satellite frequency/time duality study and capacity optimization," *Journal of Communications and Networks*, vol. 13, no. 5, pp. 472–480, 2011.
[12] J. Anzalchi, A. Couchman, *et al.*, "Beam hopping in multibeam broadband satellite systems: System simulation and performance comparison with non-hopped systems," in *2010 5th Advanced Satellite Multimedia Systems Conference and the 11th Signal Processing for Space Communications Workshop (ASMS-SPSC)*, pp. 248–255. IEEE, 2010.
[13] C. Zhang, X. Zhao, *et al.*, "Joint precoding schemes for flexible resource allocation in high throughput satellite systems based on beam hopping," *China Communications*, vol. 18, no. 9, pp. 48–61, 2021.
[14] J. Tang, D. Bian, *et al.*, "Resource allocation for leo beam-hopping satellites in a spectrum sharing scenario," *IEEE Access*, vol. 9, pp. 56 468–56 478, 2021.
[15] Z. Lin, Z. Ni, *et al.*, "Dynamic beam pattern and bandwidth allocation based on multi-agent deep reinforcement learning for beam hopping satellite systems," *IEEE Transactions on Vehicular Technology*, vol. 71, no. 4, pp. 3917–3930, 2022.
[16] J. Tang, D. Bian, *et al.*, "Optimization method of dynamic beam position for leo beam-hopping satellite communication systems," *IEEE Access*, vol. 9, pp. 57 578–57 588, 2021.
[17] B. Liu, C. Jiang, *et al.*, "Joint user grouping and beamwidth optimization for satellite multicast with phased array antennas," in *2020 IEEE Global Communications Conference (GLOBECOM)*, pp. 1–6. IEEE, 2020.
[18] C. Qi, H. Chen, *et al.*, "Energy efficient multicast precoding for multiuser multibeam satellite communications," *IEEE Wireless Communications Letters*, vol. 9, no. 4, pp. 567–570, 2019.
[19] S. K. Sharma, S. Chatzinotas, *et al.*, "Cognitive beamhopping for spectral coexistence of multibeam satellites," *International Journal of Satellite Communications and Networking*, vol. 33, no. 1, pp. 69–91, 2015.
[20] V. Bui, T. Van Chien, *et al.*, "Joint beam placement and load balancing optimization for non-geostationary satellite systems," in *2022 IEEE International Mediterranean Conference on Communications and Networking (MeditCom)*, pp. 316–321. IEEE, 2022.
[21] S. J. Orfanidis, "Electromagnetic waves and antennas," http://ecewb1.rutgers.edu/~orfanidi/ewa/, 2002.
[22] E. Welzl, *Smallest enclosing disks (balls and ellipsoids)*, pp. 359–370. Springer, 1991.
[23] Z. Drezner, "The p-centre problem—heuristic and optimal algorithms," *Journal of the Operational Research Society*, vol. 35, no. 8, pp. 741–748, 1984.
[24] A. Morello and V. Mignone, "Dvb-s2: The second generation standard for satellite broad-band services," *Proceedings of the IEEE*, vol. 94, no. 1, pp. 210–227, 2006.
[25] M. Grant, S. Boyd, *et al.*, "Cvx: Matlab software for disciplined convex programming," http://cvxr.com/cvx, 2008.

Biographies

Leyi Lyu received the B.S. degree from Nanjing University of Science and Technology, China, in 2022. She is currently pursuing her M.S. degree in signal processing from Southeast University, Nanjing, China. Her research interests include millimeter wave communications and satellite communications.

Chenhao Qi is a Professor with the School of Information Science and Engineering, Southeast University, Nanjing, China. He is the Director of Jiangsu Multimedia Communication and Sensing Technology Engineering Research Center. He is also with the National Mobile Communications Research Lab. His research interests mainly include integrated sensing and communication, millimeter wave communications and satellite communications.